Agri. & Biosys. Eng. Vol. 1(2):73-80(2000)

Evaluation of Computational Fluid Dynamics for Analysis of Aerodynamics in Naturally Ventilated Multi-span Greenhouse

I. B. Lee, T. H. Short, S. Sase, S. K. Lee

Abstract: Aerodynamics in a naturally ventilated multi-span greenhouse with plants was analyzed numerically by the computational fluid dynamics (CFD) simulation. To investigate the potential application of CFD techniques to greenhouse design and analysis, the numerical results of the CFD model were compared with the results of a steady-state mass and energy balance numerical model. Assuming the results of the mass and energy balance model as the standard, reasonably good agreement was obtained between the natural ventilation rates computed by the CFD numerical model and the mass and energy balance model. The steady-state CFD model during a sunny day showed negative errors as high as 15% in the morning and comparable positive errors in the afternoon. Such errors assumed to be due to heat storage in the floor, benches, and greenhouse structure. For a west wind of 2.5 m s^{-1}, the internal nonporous shading screens that opened to the east were predicted to have a 15.6% better air exchange rate than opened to the west. It was generally predicted that the presence of nonporous internal shading screens significantly reduced natural ventilation if the horizontal opening of the screen for each span was smaller that the effective roof vent opening.

Keywords: Computational Fluid Dynamics, Greenhouse, Ventilation, Shading Screen

Introduction

While fan ventilation of greenhouse is typically achieved with one wall as an inlet and the opposite wall as a fan outlet, natural ventilation is generally achieved by air exchanges that occur through multiple controlled openings due to natural pressure variations inside and outside the greenhouse. Natural ventilation systems of greenhouses are, therefore, very difficult to design properly while generally requiring less electrical energy, less equipment operation and maintenance, and are much quieter than fan ventilation systems.

The capability to accurately predict flow behavior within greenhouses must be significant benefit to greenhouse structural design and analysis as well as the design of heating, cooling, and ventilating systems in greenhouses. Computational fluid dynamics (CFD) simulations can be a valuable tool for analyzing the internal airflow, air temperature, humidity, and CO_2 concentration and understanding the functionality of the greenhouse structural characteristics with respect to ventilation. While CFD will never replace the need for testing, the increased importance of CFD in the analytical and design process seems assured by the rapid increase of power and decrease in the cost of computing.

The objective of this study was to verify that the CFD numerical simulations could accurately describe the airflow in a naturally ventilated multi-span greenhouse. Additionally, since the internal, retractable screen had so many positive characteristics, the influences of internal, horizontal shading screens on the natural ventilation rates and airflow patterns in the greenhouse were also studied by using CFD techniques. This study utilized the CFD model Fluent 4.5 (Fluent Inc., Lebanon, NH, USA). The computed natural ventilation rates of the two-dimensional CFD models were compared with those of a steady-state mass and energy balance model. In the mass and energy balance model, the greenhouse was considered simply as a control volume because more detail models might cause bigger errors without very extensively and accurately measured data. The experimental greenhouse used in this study was a four and one-half span, double polyethylene naturally ventilated commercial greenhouse at Quailcrest farm located near Wooster, Ohio.

Literature Reviews

Okushima et al. (1989) used an early version of a CFD model to predict the distributions of climatic factors inside and outside small naturally ventilated greenhouses. To investigate the CFD validity, the computed airflow distributions of the CFD numerical

The authors are **In Bok Lee**, STA Fellow, Laboratory of Environmental Controls in Agricultural Buildings, National Research Institute of Agricultural Engineering, Tsukuba, Japan; **Ted H. Short**, Professor, Dept. of Food, Agricultural, and Biological Engineering, The Ohio State University, Columbus, OH, USA; **Sadanori Sase**, Head of lab, Laboratory of Environmental Controls in Agricultural Buildings, National Research Institute of Agricultural Engineering, Tsukuba, Japan; **Seung Kee Lee**, Professor, Dept. of Agricultural Engineering, Kongju National University, Kongju, Korea. **Corresponding author:** In Bok Lee, STA Fellow, Laboratory of Environmental Controls in Agricultural Buildings, National Research Institute of Agricultural Engineering, Tsukuba 305-8609, Japan. e-mail: ilee@nkk.affrc.go.jp

model were compared with wind-tunnel results of Sase et al. (1984). While the experimental results showed little correlation with the computational model, the study demonstrated the possibility of using a CFD model to predict environmental distributions for naturally ventilated greenhouses. Nevertheless, CFD simulations were not used again for studying greenhouse ventilation because of the low computational capability of CFD program and limited computing power available at that time. Especially, they failed to describe in detail the effects of fluctuating turbulent airflow on the air exchange of the greenhouses with their CFD model.

Mistriotis et al. (1997) analyzed the ventilation process in un-cropped greenhouses with a CFD model. They investigated the validation of the CFD model by comparing the numerically found airflow patterns with the experimental results of Sase et al. (1984). Another quantitative test of the CFD model was performed on a twin-span Mediterranean-type greenhouse which was experimentally studied by Boulard et al. (1997). In this study, the measured and CFD computed transverse horizontal component of the average air velocity and the mean value of its fluctuation were compared each other. Good agreement between the numerical data and the experimental measurements was found when a two-scale k-ε turbulence model was used in the CFD simulation. The error, however, became larger when the experimental values included the turbulent component of the wind.

Kacira et al. (1997), Lee and Short (2000a), and Lee et al. (2000b) studied various naturally and mechanically ventilated greenhouse types by using a CFD numerical model. They mainly investigated the effects of weather conditions, greenhouse structural specifications, number of greenhouse spans, and presence of plants and benches on the air exchange rates in greenhouses.

Lee and Short (2000c, SE1763 which is decided to be published) numerically analyzed the temperature distribution in a naturally ventilated multi-span greenhouse with plants by a CFD simulation program using the standard k-ε turbulence model. The computed CFD results of air temperature distribution showed a maximum error of $\pm$3.2% for west and east winds compared to air temperatures measured in the greenhouse for the same boundary conditions. The measured air temperature distribution showed that the air came into the greenhouse through the leeward side vent opening for low wind speed.

Materials and Methods

1. Greenhouse configuration and measurements

The actual data were collected on July 16, 1997 at a double polyethylene, multi-span greenhouse designed with a windward side vent and leeward roof vents for achieving maximum ventilation with a west wind (fig. 1). It was built near Wooster, Ohio at Quailcrest farm (40° 47'N, 81° 55'W, elevation 310m). The vertical opening sizes of the side and roof vents were 0.91 m and 0.76 m, respectively. The roof cover and west wall of the greenhouse were double layer polyethylene; the south and north end walls were 8 mm polycarbonate; and, the east side wall was single layer glass. The roof was painted white with a commercial compound for shading. For convenience, the full spans were called the first, second, third, and fourth span from west to east. The partial span on the west side

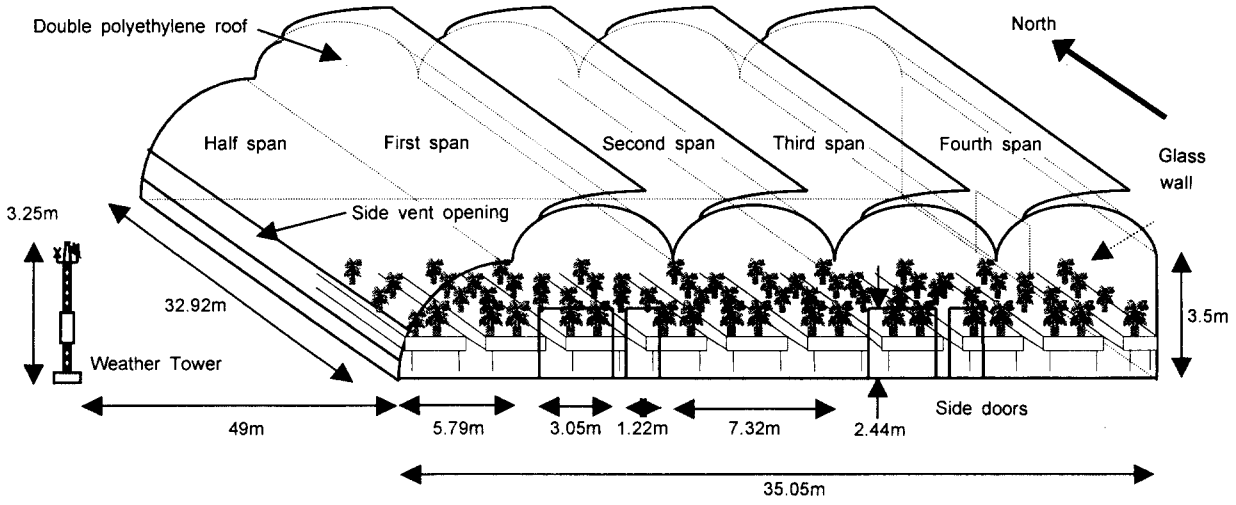

Fig. 1 A sketch of the four and one-half span naturally ventilated commercial greenhouse used in this study where the west wall and the outside weather station are to the left of the figure. All side doors were closed during data dollection.

was generally called a half span even though it was wider than half of a full span.

Ten growing benches running north-south were spaced evenly from west to east. The bottom of the benches were 0.7m from the concrete floor, and the thickness and the width of each bench were 0.2m and 2.56m respectively. The bottom of the bench was made of expanded metal to allow vertical airflow between the potted plants.

The measurements included six data collection points of air wet bulb and air dry bulb temperatures, two leaf temperature sensors (Type T-thermocouples with a wire diameter of 0.127mm and Teflon insulation, OMEGA Inc.), and one solar radiation sensor (Eppley black and white pyranometer, Model 8-48, Serial no. 14831, the Eppley Laboratory, Inc.). Aspirated dry and wet bulb temperature sensors were installed evenly across the greenhouse from the west sidewall to the east sidewall. Three sensors were installed along the length and center of the second span from north to south. The wet and drybulb temperature sensors were installed just above the plant canopy. The pyranometer was installed at gutter height in the center of the second span. Choosing a plant at the center of the greenhouse, the leaf temperature sensors were inserted into the lower side of a leaf vein at two levels and different orientations of the leaf.

While the datalogger recorded every minute, the roof cover and ground temperatures were measured every ten minutes by a portable infrared gun sensor (Raynger II Data System, ±1% accuracy). A weather station tower (3.25m height) was installed outside the greenhouse to measure the local weather such as dry and wet bulb temperatures, wind speed (Met-One Cup anemometer, Model 014A, Campbell Scientic, Inc.), wind direction (Net-one, Model 024A, Campbell Scientic, Inc.), and solar radiation.

2. Steady-state CFD numerical model

The CFD technique numerically solves the Reynolds-averaged form of the Navier-Stokes equations within each cell in a domain. The governing equations were discretized on a curvilinear grid to enable computations in complex and irregular geometry. The Reynolds-averaged process considers the instantaneous fluid velocity to be the sum of a mean and a fluctuating component, the turbulence. Since the high-frequency and small scale fluctuations of turbulent flow can not be directly quantified, turbulence numerical modeling relates some or all of the turbulent velocity fluctuations to the mean flow quantities and their gradients. The governing equations of mass, momentum, and energy used in Fluent (Launder and Spalding, 1974; Fluent manual, 1999) are briefly described in eqs. (1), (2), and (6), respectively.

$$\frac{\partial \rho}{\partial t} + \frac{\partial}{\partial x_i}(\rho u_i) = 0 \tag{1}$$

$$\frac{\partial}{\partial t}(\rho u_i) + \frac{\partial}{\partial x_j}(\rho u_i u_j) = -\frac{\partial P}{\partial x_i} + \frac{\partial \tau_{ij}}{\partial x_j} + \rho g_i \tag{2}$$

where P is the static pressure, τ_{ij} is the viscous stress tensor, and g_i is the gravitational acceleration. μ is the molecular viscosity and the second term on the right hand side is the effect of volume dilation.

$$h = \sum_{i'} m_{i'} h_{i'} \tag{3}$$

where

$$h_{i'} = \int_{T_{ref}}^{T} c_{p,i'} dT \tag{4}$$

where h is the static enthalpy, T_{ref} is a reference temperature and $C_{p,i'}$ is the specific heat at constant pressure of species i'. It is assumed that diffusion due to pressure and external forces is negligible (Fluent manual, 1999). Under this assumption, the energy equation cast in terms of h can be written:

$$\frac{\partial}{\partial t}(\rho h) + \frac{\partial}{\partial x_i}(\rho u_i h) = \frac{\partial}{\partial x_i}\left(k \frac{\partial T}{\partial x_i}\right) - \frac{\partial}{\partial x_i}\sum_{j'} h_{j'} J_{j'} + \frac{\partial P}{\partial T} + u_i \frac{\partial P}{\partial x_i} + \tau_{ij} \frac{\partial u_i}{\partial x_j} \tag{5}$$

where T is the temperature, J_j' is the flux of species j', and k is the mixture thermal conductivity.

In this study, the standard k-ε turbulence model was used because its results were observed to be most typical to known ventilation flows. The inlet airflow was assumed to be incompressible, vertically uniform in speed, and all computations were performed assuming steady-state conditions because of limited data collecting points at the weather station. The turbulent kinetic energy (k) and its rate of dissipation (ε) are obtained from the following transport equations:

$$\rho \frac{Dk}{Dt} = \frac{\partial}{\partial x_i}\left[\left(\mu + \frac{\mu_t}{\sigma_k}\right)\frac{\partial k}{\partial x_i}\right] + G_k + G_b - \rho\varepsilon - Y_M \tag{6}$$

$$\rho \frac{D\varepsilon}{Dt} = \frac{\partial}{\partial x_i}\left[\left(\mu + \frac{\mu_t}{\sigma_\varepsilon}\right)\frac{\partial \varepsilon}{\partial x_i}\right] + C_{1\varepsilon}\frac{\varepsilon}{k}\left(G_k + C_{3\varepsilon}G_b\right) - C_{2\varepsilon}\rho\frac{\varepsilon^2}{k} \tag{7}$$

In these equations, G_k represents the generation of turbulent kinetic energy due to the mean velocity gradients. G_b is the generation of turbulent kinetic energy due to buoyancy. Y_M represents the contribution of the fluctuating dilatation in turbulence to the overall dissipation rate. $C_{1\varepsilon}$(1.44), $C_{2\varepsilon}$(1.92), and $C_{3\varepsilon}$(0.09) are constants. σ_k(1.0) and σ_ε(1.3) are the turbulent Prandtl numbers for k and ε, respectively (Launder and Spalding, 1974).

3. Steady-state mass and energy balance model

Eqs. (8) and (9) present mass and energy balances respectively developed for the multi-span greenhouse using a control volume approach (Incropera and Witt, 1989; Moran and Shapiro, 1992).

$$\frac{dm_{cv}}{dt} = \sum_{k} m_{i,k} - \sum_{\lambda} m_{o,\lambda} \tag{8}$$

$$\frac{dE_{cv}}{dt} = Q_{cv} - W_{cv} + \sum_{k} m_{i,k}\left(h_{i,k} + \frac{v_{i,k}^{2}}{2} + gz_{i,k}\right) - \sum_{\lambda} m_{o,\lambda}\left(h_{o,\lambda} + \frac{v_{o,\lambda}^{2}}{2} + gz_{o,\lambda}\right) \tag{9}$$

where *cv*, *i*, and *o* were the indices for control volume, inlet, and outlet, respectively. Variables *k* and λ were components of inlets and outlets, respectively. The side vent and four roof vent openings of the greenhouse were inlet and outlets, respectively for west wind. *E*, *Q*, *W*, *h*, *v*, *g*, and *z* were energy (J), heat transfer rate (J), rate of work (J), enthalpy ($kJkg^{-1}$), velocity (ms^{-1}), acceleration of gravity (ms^{-2}), elevation (m), respectively. For steady state conditions, no accumulation of mass should occur within the control volume, such that $dm_{cv} / d_t = 0$. Then, the conservation of mass equation can be written as:

$$\sum_{k} m_{i,k} = \sum_{\lambda} m_{o,\lambda} = m_{cv} = \rho AV \tag{10}$$

where ρ, *A*, and *V* were air density (kgm^{-3}), vent opening area (m^2), and air velocity at vent opening (ms^{-1}), respectively. Further, kinetic and potential energy terms and the work term, W_{cv}, were assumed to be negligible. At steady state conditions, $dE_{cv} / dt = 0$ and an energy balance for the control volume of the greenhouse, eq. (9), becomes:

$$Q_{solar} - Q_{cover} + m_{cv}(h_i - h_o) = 0 \tag{11}$$

where Q_{solar}, Q_{cover}, m_{cv}, and *h* were solar energy available inside greenhouse ($Js^{-1}m^{-2}$), conductive heat transfer through the greenhouse cover ($Js^{-1}m^{-2}$), mass flow (kgs^{-1}), and enthalpy ($kJkg^{-1}$), respectively. Combining eqs. (10) and (11) and solving for the volumetric natural ventilation rate (AV, m^3s^{-1}),

$$AV = \frac{Q_{solar} - Q_{cover}}{\rho(h_o - h_i)} \tag{12}$$

The heat storage term was not considered in this steady-state mass and energy balance model because the steady-state model could not accurately predict the storage terms. It was assumed that 90% of solar radiation (Q_{solar}) measured inside the greenhouse was absorbed by the plant canopy (Monteith, 1990; Oke, 1991). The latent heat calculated from an equation presented by Fynn et al. (1993) was also deducted from Q_{solar}. While the balance model was the simplest, assuming the results of the mass and energy balance model as the standard, the error between the volumetric natural ventilation rates of the CFD model and the control volume energy balance model for steady state condition was calculated using:

$$Error = \frac{AV_{CFD} - AV_{E.B.}}{AV_{E.B.}} \tag{13}$$

Rewritten in terms of measured variables, eq. (13) became:

$$Error(t) = \frac{\int_{\Delta t} \rho(h_{out} - h_{in}) AV_{CFD} - \int_{\Delta t}(Q_{solar} - Q_{cover})}{\int_{\Delta t}(Q_{solar} - Q_{cover})} \tag{14}$$

If the heat storage term in the greenhouse is significant, the error term can be calculated as:

$$Error'(t) = \frac{\int_{\Delta t} \rho(h_{out} - h_{in}) AV_{CFD} - \int_{\Delta t}(Q_{solar} - Q_{cover} - Q_{stored})}{\int_{\Delta t}(Q_{solar} - Q_{cover} - Q_{stored})} \tag{15}$$

Substituting eq. (15) into eq. (14) and solving for the heat storage term,

$$Q_{stored} = \frac{(Error'(t) - Error(t))}{1 + Error'(t)}\left(Q_{solar} - Q_{cover}\right) \tag{16}$$

And if Error'(t) was assumed to be zero, then:

$$Q_{stored} = -Error(t)\left(Q_{solar} - Q_{cover}\right) \tag{17}$$

4. Experimental and theoretical procedures

The volumetric ventilation rates from the CFD model and the mass and energy balance model were compared to each other to verify the accuracy of the CFD simulation. The validity of the CFD model was investigated for clear sky conditions from 8:30AM to 5:00PM on July 16, 1997. The wind direction was mostly perpendicular to the west side vent of the greenhouse which was the essential for the two-dimensional CFD models. Since the data significantly fluctuated during collection, data were collected every minute and averaged every 15 minutes. The average weather data were used as the input data for both the CFD model and the mass and energy balance model.

All side doors of the greenhouse were totally closed during data collection. The time used throughout the study was Eastern Daylight Saving Time (EDST) and was referred to as local time.

The effect of internal shading screens on natural ventilation of the multi-span greenhouse was also investigated using the CFD models with 2.5 m s^{-1} of west wind. This test was conducted without any plants in the greenhouse, and it was assumed that the internal, horizontal shading screens had zero porosity. A porous media utility with 0.0 porosity was developed as the shading screen in the computational CFD model. The effects of the internal and horizontal shading screens on ventilation air exchange rate (G.V. min^{-1}) were investigated for being opened to both the east and west. The case studies of different percent of shaded area were 0%, 25%, 50%, 75%, 80%, 85%, 90%, 95%, and 100% when the horizontal width of the unshaded area for each span was 7.44 m, 5.61 m, 3.78 m, 1.95 m, 1.58 m, 1.22 m, 0.85 m, 0.49 m, and 0.12 m, respectively. The shaded area for each span indicated the ratio of the shading screen area to the floor area. The 100% shading still had 0.12m of horizontal opening for each span because, under each gutter, there was small opening gap between the adjacent cables supporting the shading screens.

Results and Discussion

1. Accuracy of CFD models

The validity of the CFD model was investigated with a steady state mass and energy balance model comparing the volumetric flow rates (m^3s^{-1}). Figs. 2 and 3 show the changes of wind speed, wind direction, and outside solar radiation, respectively with standard deviations from 8:30 AM to 5:00 PM EDST on July 16, 1997. The average wind speed and direction were 2.35 ms^{-1} and 246.9 degrees, respectively with the wind speed gradually increasing during the day. The sky was clear in the morning making the solar radiation very stable. During the afternoon, however, the solar radiation was unstable due to clouds.

Fig. 4 shows the predicted volumetric flow rates of the CFD model in comparison to the mass and energy balance model. It indicated that the volumetric flow rate of the CFD model gradually increased as the wind speed increased during data collection. The results of the CFD model were significantly related to the wind speed with R^2 value of 0.9715. Assuming the results of the mass and energy balance model as the standard, fig. 4 shows mostly negative errors in the morning and positive errors in the afternoon. Assuming that the values in eq. (12) were accurately measured, the solar energy (Q_{solar}) in the greenhouse might be over-estimated in the morning due to heat storage in the floor, benches, and greenhouse structure. When the

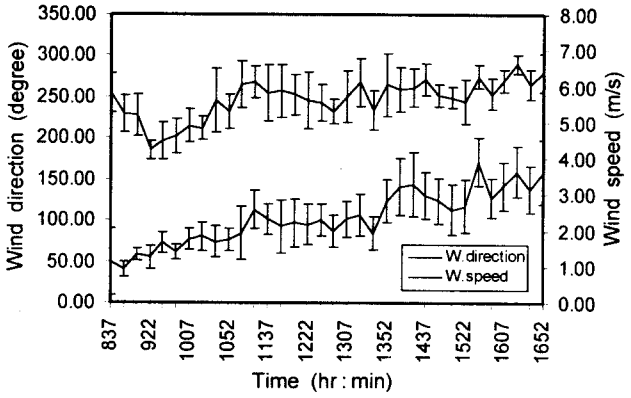

Fig. 2 Average wind speed and direction from 8:30AM to 5:00PM EDST (July 16, 1997) with standard deviations calculated for each 15 minutes. The wind direction sensor indicated north, east, south, and west as 0, 90, 180, and 270, respectively.

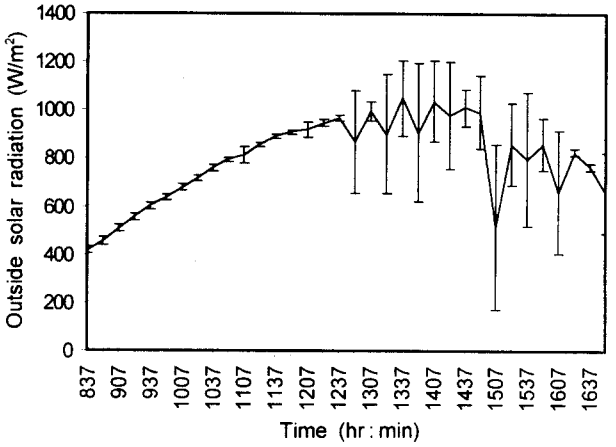

Fig. 3 Average outside solar radiation from 8:30AM to 5:00PM EDST (July 16, 1997) with standard deviations calculated for each 15 minutes.

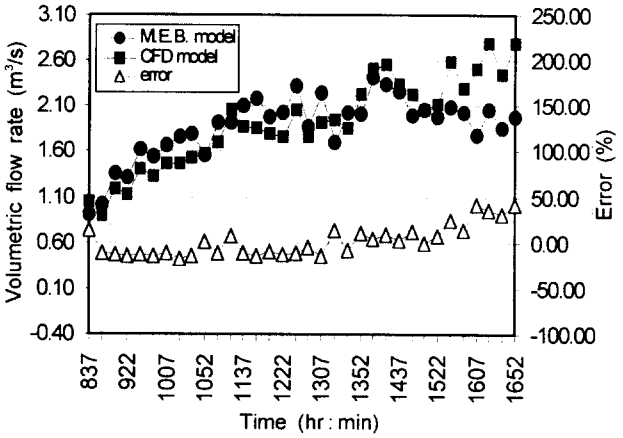

Fig. 4 The volumetric flow rates (m^3 s−1) of the CFD model and the mass and energy balance model as well as the errors between two models for each time period from 8:30AM to 5:00PM EDST (July 16, 1997).

solar radiation decreased and the wind speed increased in the afternoon, the stored heat might have been released inside greenhouse volume and the error became positive as shown in fig. 4. The air temperature differences between inside and outside the greenhouse throughout the day indicated that the temperature difference did not decrease in the late afternoon even though the wind speed increased and the solar radiation decreased as shown in figs. 2 and 3. It indicated that there was significant heat storage effect.

By using eq. (17), the heat storage flux in the greenhouse was predicted and illustrated in fig. 5 along with the solar energy in the greenhouse, conductive heat transfer through the greenhouse cover, and ventilated heat transfer from 8:30AM to 5:00PM EDST. In fig. 5, it was predicted that the first calculated heat storage term was negative in the early morning. It was observed that the roof vents were closed until approximately 8:30AM after which they were fully opened allowing heat stored in the greenhouse to be released. Conductive heat losses were never significant as compared to the other thermal energies because of small temperature differences between inside and outside the greenhouse. Heat loss by natural ventilation gradually increased as the wind speed increased. The calculated Error(t) represented the ratio of the heat stored in greenhouse to net energy entering the greenhouse. Fig. 5 shows that about 15 % of the net energy entering the greenhouse were being stored in the morning while, in the afternoon, heat energy was being lost from storage.

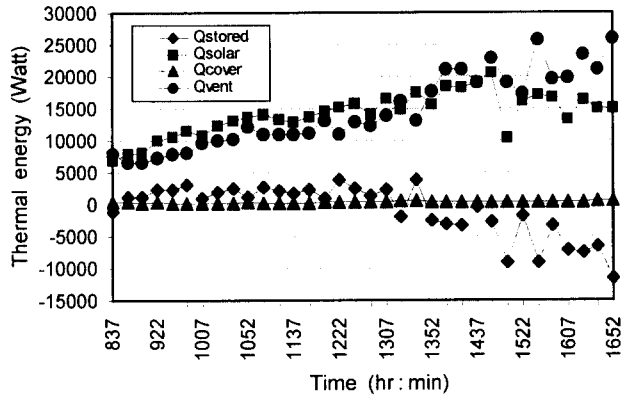

Fig. 5 The changes of predicted thermal energies in the greenhouse for each time period from 8:30AM to 5:00PM EDST. Q_{stored}, Q_{solar}, Q_{cover}, and Q_{vent} indicated stored heat energy, solar energy, conductive heat transfer through cover, and ventilated heat transfer through opening, respectively.

Considering the ASAE Standard (1998) of 0.75 ~ 1.0 volume per minute (G.V. min^{-1}) for a fan ventilation system, the CFD computed results showed that the four and one-half span greenhouse could achieve an optimum ventilation rate of 0.75 G.V. min^{-1} when the wind speed from the west was 2.4 ms^{-1}.

2. Effect of internal shading screens on natural ventilation

Table 1 shows the predicted volumetric flow rates at the vent openings according to the percentage of shaded area and opening direction of shading screens for a west wind of 2.5 m s^{-1}. When the shaded area was less than 90%, the air mainly was predicted to move in through the side vent and the first roof vent opening and move out through all roof vent openings. The side vent opening acted as a main inlet of airflow and the fourth roof vent was the most effective opening among the roof vents as an outlet. The predicted volumetric airflows at roof vent openings were much more uniform when the shading screens were opened to the east and the shading area was less than 90%. When the shaded area was 95%, the air was predicted to move in through the side vent and move out through all the roof vent openings.

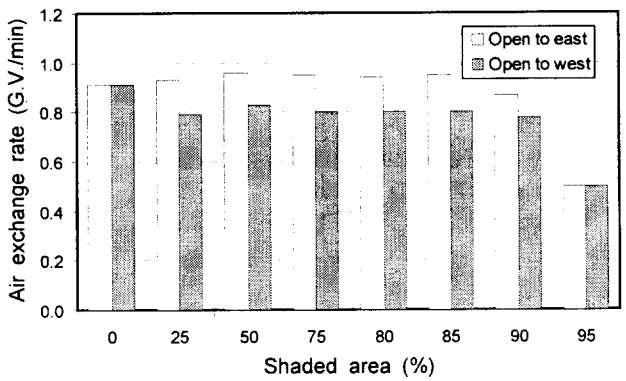

Fig. 6 A comparison of the air exchange rates when the shading screens were opened to the east and west with a west wind of 2.5 ms^{-1}.

The predicted volumetric air exchange rates were compared according to the percentage of shaded area and opening direction of shading screens for a west wind of 2.5 m s^{-1} shown in fig. 6. The figure shows that the internal nonporous shading screens that opened to the east were predicted to have a 15.6% better air exchange rate than opened to the west. The results also showed that the predicted air exchange rates were significantly influenced by the change of shaded area when the percentage of shaded area was more than 90 %. When the shading screens were opened to the east and the shaded area was less than 90%, all the cases achieved a recommended air exchange rate greater than 0.75 G.V. min^{-1} according to ASAE Standard (1998). The predicted air exchange rate was the highest (0.96 G.V. min^{-1}) when the shaded area for each span was

Table 1 The effect of the percentages of shading screens on natural ventilation in greenhouse when the screen was opened to the east and west with a west wind of 2.5 ms^{-1}.

Opened to	Shade area (%)	Volumetric flow rate (m^3s^{-1}), inlet/outlet				
		Side vent	Roof 1	Roof 2	Roof 3	Roof 4
East	0	2.32/0.00	0.25/0.09	0.00/0.31	0.00/0.70	0.00/1.28
	25	2.34/0.00	0.27/0.09	0.00/0.27	0.00/0.68	0.00/1.39
	50	2.36/0.00	0.33/0.08	0.00/0.21	0.00/0.71	0.00/1.50
	75	2.36/0.00	0.30/0.09	0.00/0.25	0.00/0.72	0.00/1.42
	80	2.35/0.00	0.28/0.09	0.00/0.28	0.00/0.72	0.00/1.37
	85	2.32/0.00	0.24/0.10	0.00/0.33	0.00/0.70	0.00/1.29
	90	2.27/0.00	0.18/0.12	0.00/0.37	0.00/0.64	0.00/1.14
	95	1.44/0.00	0.00/0.28	0.00/0.38	0.00/0.48	0.00/0.34
West	0	2.32/0.00	0.25/0.09	0.00/0.31	0.00/0.70	0.00/1.28
	25	2.20/0.00	0.03/0.03	0.00/0.27	0.00/0.55	0.00/1.18
	50	2.26/0.00	0.08/0.03	0.00/0.29	0.00/0.60	0.00/1.23
	75	2.18/0.00	0.06/0.06	0.01/0.33	0.00/0.59	0.00/1.12
	80	2.14/0.00	0.04/0.10	0.01/0.38	0.00/0.57	0.00/0.96
	85	2.15/0.00	0.07/0.08	0.01/0.39	0.00/0.59	0.00/1.05
	90	1.92/0.00	0.20/0.11	0.07/0.16	0.00/0.65	0.00/1.10
	95	1.31/0.00	0.02/0.29	0.00/0.44	0.06/0.15	0.04/0.41

50% while the air exchange rate was 0.91 G.V. min^{-1} when the shaded areas were 0%. When the shading screens were opened to the west, the predicted air exchange rates of all the shaded cases were lower than the air exchange rate of no shaded case. The predicted air exchange rate was the highest among those shaded cases when the shaded area was 50%.

Fig. 6 would indicate that the presence of the shading screen influenced the natural ventilation rate if the horizontal width of the unshaded area for each span was smaller than the vertical width of the roof vent openings. If the horizontal width of the unshaded area for each span was bigger than the width of the roof vent, the air exchange rate was predicted to be unaffected by the change of shaded area. The vertical opening sizes of the side and roof vents were 0.91 m and 0.76 m, respectively.

Fig. 7 shows the CFD predicted contours of the airflow in the computational domains when the shading screens (50% covered) were opened to the east (a) and west (b) with a west wind of 2.5 ms^{-1}. The figures show that the airflow followed the smooth roofline and moved toward the leeward roof vent openings when the shading screens were opened to the east. It was assumed that the shading screens opening to the west interrupted the smooth airflow to the roof vent more than the shading screens opening to the east shown in

(a) Opened to the east

(b) Opened to the west

Fig. 7 The CFD predicted contours of the airflows in the computational domains when the shading screen (50% covered) were opened to (a) east and (b) west with a west wind of 2.5ms^{-1}. The maximum and minimum air speeds in the computational domains were (a) 4.36 ms^{-1} and 0.004 ms^{-1}, respectively and (b) 4.28 ms^{-1} and 0.003 ms^{-1}, respectively. The darker indicates the high wind speed.

fig. 7. When the shading screens were opened to the east, the strong inlet air stream through the side vent was predicted to develop air circulation below the first roof and help the inlet airflow through the first roof vent opening. The figures also show that the fourth span was predicted to not ventilate well when the shading screens were opened to the east.

Conclusions

The results of the mass and energy balance model were mainly influenced by solar energy and enthalpy difference between inside and outside the greenhouse. For the CFD model, the most significant factor was the wind speed at a correlation coefficient of 0.9715.

Assuming the results of the mass and energy balance model as the standard, reasonably good agreement was obtained between the natural ventilation rates computed by the CFD numerical model and the mass and energy balance model. The steady state CFD model during a sunny day showed negative errors as high as 15% in the morning and comparable positive errors in the afternoon. Such errors assumed to be due to heat storage in the floor, benches, and greenhouse structure.

Considering the ASAE Standard (1997) of 0.75 - 1.0 volume per minute (G.V. min^{-1}) for a fan ventilation system, the CFD computed results showed that the four and one-half span greenhouse could achieve an optimum ventilation rate of 0.75 G.V. min^{-1} when the wind speed from the west was 2.4 ms^{-1}.

For the airflow studied, the side vent and the fourth roof vent openings were predicted to have the largest volumetric airflows as inlet and outlet, respectively. The air circulation patterns in the greenhouse were predicted to be significantly influenced by both the shading system and vent openings.

For a west wind of 2.5 ms^{-1}, the internal nonporous shading screens that opened to the east were predicted to have a 15.6% better air exchange rate than opened to the west. It was shown that the shading screens opened to the west could potentially interrupt the smooth airflow to the roof vents more than the shading screens opened to the east. The predicted air exchange rate was the highest when the shaded area for each span was 50%.

For both opened directions of shading screens, acceptable air exchange rates were predicted when the percentage of shaded area for each span was less than 90%. It was generally predicted that the presence of shading screens could influence the natural ventilation if the horizontal width of the unshaded area for each span was smaller than the effective opening width of the roof vent openings.

References

ASAE Standard. 1998. ASAE Engineering Practice : ASAE EP406, ASAE Standard-1998, American Society of Agricultural Engineers, St. Joseph, MI 49085.

Boulard, T., F. J. Meneses, M. Mermier and G. Papadakis. 1997. The mechanisms involved in the natural ventilation of greenhouses. Agricultural and Forest Meteorology. 79:61-77.

Fluent company. 1999. The manual of Computational Fluid Dynamics (CFD), Version 4.5, Lebanon, NH 03766.

Fynn, R. P., A. Al-shooshan, T. Short and R. McMahon. 1993. Evapotranspiration measurement and modeling for a potted chrysanthemum crop. Transactions of the ASAE, 36:1907-1913.

Incropera, F. P. and D. P. Witt. 1989. Introduction to heat transfer, Second edition. John wiley & sons, Inc., New York.

Kacira, M., T. Short and R. Stowell. 1998. A CFD evaluation of naturally ventilated, multi-span, sawtooth greenhouses. Transactions of the ASAE, 41:833-836.

Launder, B. E. and D. B. Spalding. 1974. The numerical computation of turbulent flows. Computer methods in applied mechanics and engineering, Vol.3:269-289.

Lee, In-Bok and T. H. Short. 2000a. Two dimensional numerical simulation of natural ventilation in a multi-span greenhouse. Transactions of ASAE, 43(3): 745-753.

Lee, In-Bok, T. H. Short, Sadanori Sase, Limi Okushima and Guo Yu Qiu. 2000b. Evaluation of structural characteristics of naturally ventilated multi- span greenhouses using computer simulation. Japanese Agricultural Research Quarterly (JARQ), 34(4):245-255.

Lee, In-Bok and T. H. Short. 2000c. Verification of computational fluid dynamics numerical simulation using for analysis of greenhouse natural ventilation. Transactions of ASAE. (in press).

Mistriotis, A., G. P. A. Bot, P. Picuno and G. Scarascia-Mugozza. 1997. Analysis of the efficiency of greenhouse ventilation using computational fluid dynamics. Agricultural and Forest Meteorology, pp1-12.

Monteith, J. L. and M. H. Unsworth. 1990. Principles of Environmental physics. Routledge, Chapman and Hall, Inc., New York.

Moran, M. J. and H. N. Shapiro. 1992. Fundamentals of engineering thermodynamics, 2nd ed., John Wiley & Sons, Inc., New York.

Oke, T. R. 1987. Boundary layer climates, 2nd ed. Routledge, Chapman and Hall, Inc., New York.

Okushima, L., S. Sase and M. Nara. 1989. A support system for natural ventilation design of greenhouses based on computational aerodynamics, Acta Horti-culture, 248:129-136.

Sase, S., T. Takakura and M. Nara. 1984. Wind tunnel testing on airflow and temperature distribution of a naturally ventilated greenhouse. Acta Horticulture, 148:329-336.